Triple photoionization of Ne and Ar near threshold

J. B. Bluett,[1] D. Lukić,[2] and R. Wehlitz[1,*]
[1]*Synchrotron Radiation Center, UW-Madison, Stoughton, Wisconsin 53589, USA*
[2]*Institute of Physics, 11001 Belgrade, Serbia and Montenegro*
(Received 24 November 2003; published 23 April 2004)

The triple-photoionization cross section of neon and argon near threshold has been investigated by ion time-of-flight spectrometry. We applied the Wannier power law to our data and confirmed the theoretical Wannier exponent in the cases of Ne and Ar. Our data also agree with previous findings regarding the Wannier exponent and its range of validity for Ne. However, the Wannier power law exhibits a much smaller range of validity of 2 eV for Ar compared to 5 eV for Ne. Also, in contrast to a previous experiment, we do not find a "second" power law but a gradual decrease of the exponent above the range of validity of the Wannier power law.

DOI: 10.1103/PhysRevA.69.042717 PACS number(s): 32.80.Fb

I. INTRODUCTION

The study of multiple-ionization processes in atoms is of fundamental importance for understanding the interactions among charged particles. Although multiple ionization appears to be a simple process, the interaction of only three charged particles cannot be described analytically but can be solved numerically [1]. This situation is usually referred to as the "three-body Coulomb problem." In the case of triple photoionization (TPI) with three simultaneously ejected electrons and one remaining ion, we actually have a four-body problem which is even less understood.

Although the interaction of charged-particle projectiles with gases is of high physical importance for ionization processes, there are distinct advantages in using photons for ionization. In contrast to charged-particle collisions, ionization by a single photon (except for Compton scattering) has a well-defined energy- and angular-momentum transfer from the projectile to the target atom and provides a simpler testing ground for theoretical models. Since the photoelectric operator is a one-electron operator, only single-electron excitation or ionization is possible within the framework of the independent-particle model. Therefore, multielectron processes are entirely due to correlation effects among electrons.

The simplest case of multiple photoionization is the double-photoionization (DPI) process in helium. Many experiments and theoretical investigations were—and still are—concerned with the DPI of He (see, e.g., Refs. [2,3]). From the periodic table, Li represents the next level of sophistication from the He problem because now TPI is possible. However, Li ($1s^2 2s$) presents a new problem due to the different binding energies of the 1*s* and 2*s* electrons [4,5]. Ne ($2s^2 2p^6$) and Ar ($3s^2 3p^6$) are again "heliumlike" because each *p* valence electron has the same binding energy, just as the 1*s* electrons of He have the same binding energy. While this is also true for other elements, e.g., aluminum, Ne and Ar are easy to handle experimentally.

Numerous multiple-photoionization experiments were performed for the noble gases Ne, Ar, Kr, and Xe, but mostly near inner-shell thresholds where Auger processes become possible. Only a few studies were concerned with the long-range, nonresonant behavior of the TPI cross section [6–10]. In these cases, however, the spectra were taken with either large energy steps or not near threshold. Triply charged photoions of elements other than noble gases were measured for Li [4], K and Ca [11], Cs and Ba [12], Ba [13], Sm and Eu [14], Mg [15], and U [16], but again this was done mainly in the region of resonances (except for Li).

The theoretical framework for multiple photoionization near threshold has been in place for decades. One of the early theories describing the double- [17] and later the multiple-ionization [18] cross sections near threshold was developed by Wannier. Wannier's theory tells us that the triple-photoionization cross section σ^{3+} follows a power law

$$\sigma^{3+} \propto E^{\alpha}, \tag{1}$$

where E is the energy above threshold and α is slightly larger than 2.0. However, this theory does not provide a range of validity for this threshold law.

According to Klar and Schlecht [19], who were the first to calculate the value of the Wannier exponent for TPI, the exponent is $\alpha = 2.162$ at threshold. This value was later confirmed by other theorists [20–25] using various methods. More general breakup processes of charged particles near threshold are discussed in Refs. [23–26].

It is worthwhile to mention that there is an alternative description of the near-threshold cross section for the direct emission of two electrons. It is the Coulomb-dipole theory which was developed by Temkin [27,28] for electron-impact ionization. However, this theory does not describe the three-electron emission.

As mentioned above, most measurements of the TPI cross section were performed far above threshold. Only for three atoms (Ne, O, and Li) the TPI process was studied near threshold [5,29]. In general, triply charged ions can be created by different photoionization processes for the energies far above threshold and Auger processes can also contribute to the production of triply charged ions. This complicates a straightforward interpretation of the data. In this respect, the

*Electronic address: wehlitz@src.wisc.edu

near threshold region is not only simpler to analyze but is also of particular interest due to the strong interactions among the ejected electrons and residual ion.

Soon after the first double-photoionization experiment near threshold [30] using He, the first triple-photoionization experiments near threshold were performed by Samson and Angel for Ne and atomic oxygen [29] at the Synchrotron Radiation Center (SRC). They confirmed the Wannier threshold law and obtained an exponent of 2.17(9) for Ne and 2.18(9) for atomic oxygen with a range of validity of about 5.0–5.5 eV for both Ne and O. The same authors also mention a "second" power law above 5.5 eV with an exponent of $\alpha=1.88$ for Ne and $\alpha=1.84$ for oxygen without error bars or a range of validity for this law. Note that their highest energy is only 9 eV above threshold. However, assuming that such a second power law does exist, a very different exponent ($\alpha=1.35$) from that of Ne and O was obtained in the case of Li [5]. For Li the second exponent is merely a numerical result without a physical basis because the energy dependence of the TPI cross section can be easily explained by a shakeoff process [5].

Nevertheless, a second power law has not only been observed in the case of Ne and O but was also found in the calculations by Feagin and Filipczyk [21]. While they have confirmed the Wannier exponent for one breakup mode of an atomic system, they have found an additional breakup mode that leads to an exponent of 1.821, which is in accord with Samson and Angle's second exponent. This situation resulted in some debate on whether the Wannier theory fully describes the TPI process near threshold and how the Wannier exponent changes when going above threshold. Kuchiev and Ostrovsky [23] do not see any possibility for an additional breakup mode and reject the idea of a second power law. It should also be mentioned that Pattard and Rost [24] have found a correction term to the Wannier power law for multiple ionization, which, however, does not apply to triple photoionization.

II. EXPERIMENT

The experiment was performed at the Aladdin storage ring of the Synchrotron Radiation Center. Monochromatized synchrotron radiation from three different beamlines, namely, the plane grating monochromator (PGM) [31], the six-meter toroidal-grating monochromator (6m-TGM) [32], and the Mark II grasshopper (Mark II) [33] beamlines, were used for the experiments.

Because the experiment required only moderate energy resolution but did require high photon flux, the monochromator entrance and exit slits could be opened relatively wide. The degree to which they were opened depended on each beamline's characteristics. The entrance and exit slits of the PGM beamline were set at 255 μm and 150 μm, respectively, yielding an energy resolution of 90 meV at 130 eV for the Ne measurements and 60 meV at 90 eV for the Ar measurements. Filters were not employed because second-order light is beyond the beamline's energy range in the case of Ne or extremely small in the case of Ar. Stray light has not been observed at this undulator beamline.

At the 6m-TGM we used the high-energy grating for the Ne measurements with both slits set at 200 μm yielding an energy resolution of 80 meV at 130 eV. For the Ar measurements we used the medium-energy grating at the same beamline with both slits set at 200 μm yielding an energy resolution of 110 meV at 90 eV. We also employed a SiN filter which has a cutoff energy of about 106 eV and suppressed second-order light. Note that we did not use a filter for the Ne experiment because any second-order light would be beyond the energy range of the grating. For all beamlines the photon energy resolution was high enough so that a convolution of the partial-ion-yield data was not necessary.

Some of the Ne measurements were performed on the Mark II beamline with both slits set at 30 μm yielding an energy resolution of 0.16 eV at 130 eV; additional apertures in the beamline were optimized to reduce stray light.

The monochromatized photon beam passed through our differential pumping stage and entered the experimental chamber filled with either Ne or Ar. The background pressure in the experimental chamber was lower than 1×10^{-8} mbar. The Ne and Ar gas pressures were 5×10^{-6} mbar and 7×10^{-6} mbar, respectively, and were easily controlled by a regulator and a needle valve attached to the chamber. We did not observe a pressure dependence in the ion-yield ratios for these sample gas pressures.

The photoions were produced where the photon beam intersected the gas and were detected with an ion time-of-flight (TOF) spectrometer operating in the pulsed extraction mode. This pulsed electrical field (20 V/cm) across the interaction region accelerated the ions towards the drift tube and provided a start signal for the flight-time measurement. The ions were detected with a Z-stack microchannel-plate (MCP) detector which provided the corresponding stop signal [34].

The TOF spectrometer is used to measure the mass-to-charge ratio of incoming ions, allowing us to resolve the target ions with different charges and measure the area of each ion peak. From these areas, we determined the triple-to-double and double-to-single ionization ratios separately. This was done because the large peak of singly charged ions caused dead time in the electronics which affected the intensity of the feeble triply charged ion peak. By using an XUV100 silicon photodiode, which has a known quantum efficiency, we calculated the relative cross section for triple photoionization, assuming that the gas pressure does not change with time.

We used a $\times10$ preamplifier to enhance the MCP pulse, and the threshold of our constant-fraction discriminator (CFD) was set to a low level ($\leqslant40$ mV) to ensure that there was no difference in the detection efficiency between the singly, doubly, and triply charged ions. This was established experimentally by measuring the DPI ratio as a function of the CFD threshold, which remained constant around the CFD threshold used during the experiments. We also looked at the DPI ratio as a function of the characteristics of the extraction pulse. Since the DPI ratio was found to be independent of pulse length and period of the extraction pulse around our set values (period =20 μs, width =2 μs), we did not discriminate against a given charge state. In order to cross-check the experimental parameters we compared our partial cross-section ratios at energies far above threshold to those of a

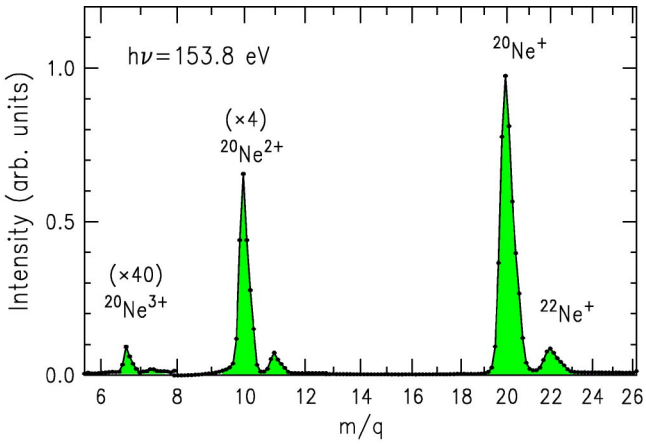

FIG. 1. Neon ion time-of-flight spectrum taken at a photon energy of 153.8 eV. Note that the *x* axis is not linear.

previous experiment [9] and found agreement within error bars.

We also took ion spectra below the TPI thresholds of Ne and Ar (125.99 eV and 84.30 eV, respectively [35]). These spectra did not reveal any appreciable amount of triply charged ions. From that we conclude that the monochromatized photon beam with the settings used for the experiments did not contain significant higher-order photon energy contributions.

III. DATA ANALYSIS

In order to determine the energy dependence of the TPI cross section, we took ion time-of-flight spectra at several photon energies near threshold. The data analysis is essentially the same for Ne and Ar. As an example, Fig. 1 shows a Ne spectrum taken at $h\nu=153.8$ eV. The areas of the ion peaks were numerically integrated, and the area of the much smaller Ne^{3+} peak was also checked for consistency by applying a least-squares fit using a Gaussian profile. A numerical integration of the Ne^{3+} peak yielded the same area as the fitting program within the error bars. The statistical error provided by the fitting program and the numerical integration corresponds to a 1σ error bar. From these areas, we calculated the triple-to-double and double-to-single photoionization ratios.

We applied an energy correction to the photon energy, which we determined by taking an ion-yield scan of Kr across the $3d_{5/2}\rightarrow 5p$ resonance, which has a well-known energy of 91.20(1) eV [36], and comparing that value to the energy we dialed into the monochromator. The energy correction was assumed to be a constant shift in wavelength over the energy range of interest, accurate within the photon beam's energy resolution. The corrections were never larger than a few hundred meV.

As a test for systematical errors, we took reference spectra at an arbitrarily chosen photon energy occasionally. We found the reference value for the triple-to-double photoionization ratio to be within the error bar except when we took data at the 6m-TGM beamline. There we found that the grating required several hours to warm up before the ratio became stable. When the grating was cold, the ratio appeared slightly higher. As the grating warmed up, the ratio approached an asymptotic limit. By graphing the ratio of the reference spectra as a function of the amount of time that had passed since the grating was exposed to photons, we were able to establish a normalization of the reference spectra. In essence, we determined the way the ratio changed as the monochromator warmed up and applied the factors in such a way that the "cold" grating data agreed with the "warm" grating data. By applying a multiplicative factor determined by the time of day the spectrum was taken, we were able to use the data where the reference spectra were outside of the error bars. This method brought the reference spectra into agreement.

Since the absolute photoabsorption cross sections σ_{tot} of Ne and Ar are known [9] we have calculated from our relative partial ion yields the absolute TPI cross section in the energy range of interest. To determine the TPI cross section $\sigma(Ne^{3+})$ we used the formula:

$$\sigma(\mathrm{Ne}^{3+}) = \frac{\sigma_{\mathrm{tot}}(h\nu)R^{3+}R^{2+}}{1+R^{2+}+R^{3+}R^{2+}}. \tag{2}$$

Here, R^{2+} and R^{3+} denote our measured double-to-single and triple-to-double photoionization ratios, respectively. Although we do not measure absolute cross sections directly, we can use the above equation to derive an absolute cross section. Here, we have used the numerically listed cross sections of Suzuki and Saito [10] which are also displayed in Ref. [9]. Since the double-to-single photoionization ratio R^{2+} is a smooth function of energy in the region around the triple-ionization threshold, we used a smooth curve through our measured ratios R^{2+} in order to minimize the statistical error.

The combined data from different beamlines were used to determine the Wannier exponent and the energy range of validity of that exponent. The formula used as a fit model was

$$\sigma(E) = \sigma_0 E^{\alpha} + C, \tag{3}$$

where σ is the TPI cross section, E is the excess energy, σ_0 is the TPI cross section at 1 eV above threshold, α is the Wannier exponent, and C is a constant background. We ascribe this background to three possible sources which contribute in different proportions at different beamlines: (a) a small second-order light contribution, (b) possible excitations by electron impact, and (c) high-energetic stray light.

Even though the second-order light contribution was suppressed by filters or deemed to be small, it may affect the small TPI cross section near threshold because of the much larger TPI cross section at twice the set photon energy. Note that the background was almost negligible for the data taken at the undulator beamline. Electron impact processes may also contribute to the very small TPI cross section. Electrons, which originate either from the gas via photoionization or from the synchrotron light hitting the back of our chamber, can hit other ions and may produce triply charged from doubly charged ions. Another source for the observed back-

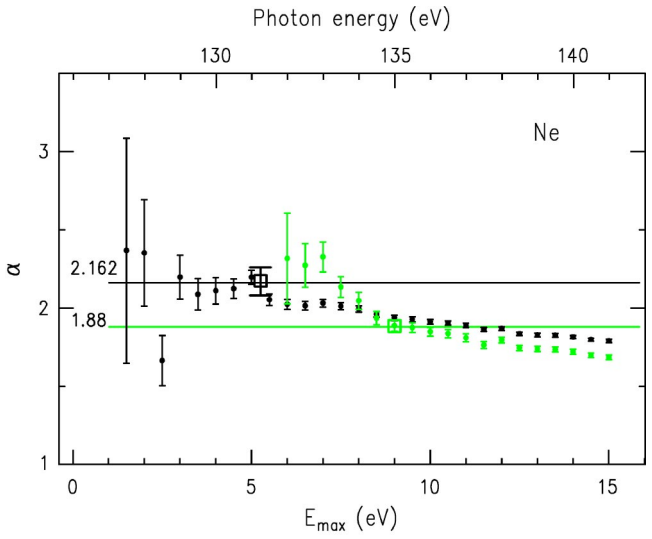

FIG. 2. The Wannier exponent α as a function of the upper limit E_{max} of the energy range over which the power-law fit was applied. The lower limit of the fit range is always 0.5 eV for the black data points and 5.0 eV for the gray data points. The black and gray open squares are the data of Samson and Angel [29] who had used only a single fit range for the lower and upper excess-energy regions. The horizontal lines indicate exponents of 2.162 and 1.88, respectively.

ground may be scattered (nonmonochromatized) synchrotron light of an energy high enough to triple ionize our sample.

The excess energy E was determined by subtracting a threshold energy of 125.99(1) eV for Ne [35] and 84.30(1) eV for Ar [35] from the corrected photon energy.

IV. NEON

We have taken Ne spectra in the photon energy range from 126 to 146 eV in small steps and analyzed the partial ion yields as described above. We used least-squares fitting of the TPI cross section according to Eq. (3), where σ_0, α, and C were allowed to vary. This fit was performed for excess-energy ranges always starting at 0.5 eV extending to an upper energy limit that increased in 0.5 eV steps. This allowed us to examine how the variables behave as a function of energy range used in the fit procedure. Naturally, a smaller fit range results in larger error bars because less data points are used for the fit. On the other hand, a too large energy range may be larger than the range of validity of the Wannier power law.

By looking at C as a function of energy range with σ_0 and α free, we noticed that C did not vary much near threshold. Since it was a relatively stable variable, we took a weighted average of these values and used that value and its corresponding uncertainty to constrain C.

Allowing σ_0 and α to vary as a function of the upper limit of the fit range, α takes on the values shown in Fig. 2. Note that the lowest energy point is the result of a fit using only two cross-section values. As the upper limit of the fit range increases, the α values become more accurate. From this figure we conclude that the energy range of validity of the

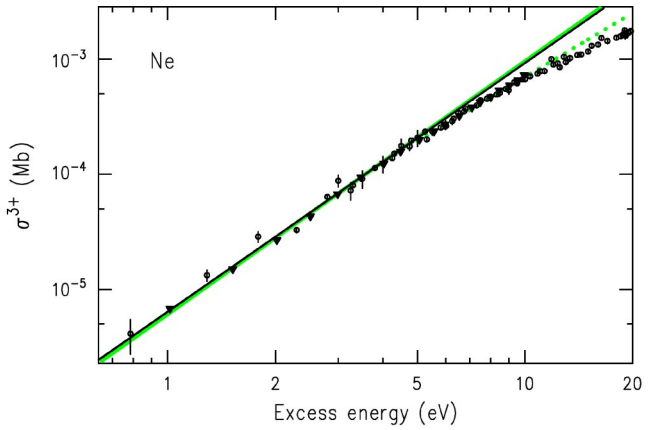

FIG. 3. Triple-photoionization cross section of Ne as a function of excess energy on a double-log scale: circles, this work; triangles, Ref. [29]. The solid black line corresponds to the theoretical exponent of 2.162 while the solid gray line is the fit curve to our data. The dotted line corresponds to a power-law fit between 5 and 9 eV.

Wannier power law extends to ~5.0 eV. Performing a single fit extending over the excess energy range from 0.0 to 5.0 eV yields an exponent of $\alpha=2.20(5)$ as shown in Fig. 3, which agrees with the previously measured value of 2.17 [29] and confirms the theoretical value of 2.162. For σ_0 we obtain a value of 6.4(3) b, which corresponds to the TPI cross section at 1 eV above threshold.

When the same fit is performed (allowing only σ_0 and α to vary while C is still the same value used above) starting at 5.0 eV, the exponent α varies as shown in gray in Fig. 2. When a fit is performed from 5.0 eV up to 9.0 eV—the highest point in energy that Samson and Angel [29] have used—we obtain an exponent $\alpha=1.89(4)$, which agrees well with Samson and Angel's value of $\alpha=1.88$. Our curve for a second power law is shown in Fig. 3. It extends from 5.0 eV to about 10 eV above threshold.

However, Fig. 2 also shows that the exponent varies as a function of energy range. It appears that the exponent *gradually* decreases from $\alpha=2.20$ with increasing energy once the near-threshold condition in the Wannier theory no longer applies. While the previously observed second exponent has been verified for a particular energy range, it is in general dependent on the energy range over which the power-law fit is performed. Unlike the Wannier exponent, which is valid for the first 5 eV above threshold, the exponent decreases steadily above that range.

It is worthwhile to mention that the deviation of the measured exponent from the theoretical Wannier exponent starts at about 5 eV and coincides with the next higher $2p^3(^2D)$ TPI threshold. However, Samson and Angel [29] found the same behavior of the exponent in the case of oxygen where no state of a similar energy exists.

V. ARGON

We have measured partial ion yields of Ar (Fig. 4) in the photon energy range from 84 to 94 eV in small steps and determined the Ar^{3+} cross section as described above. Using

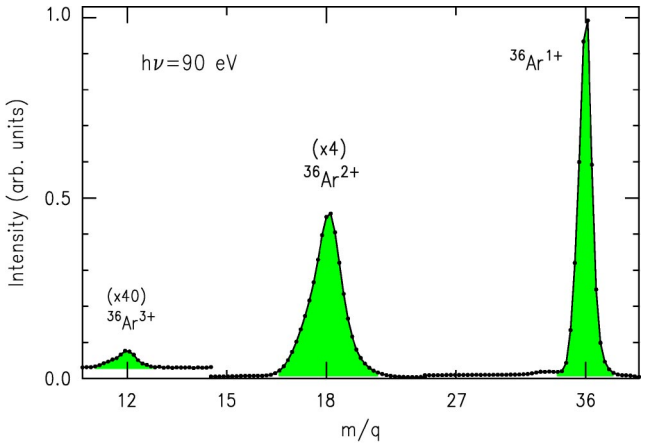

FIG. 4. Argon ion time-of-flight spectrum taken at a photon energy of 90 eV. Note that the *x* axis is not linear.

the same fit model as we did for the Ne^{3+} partial cross section [Eq. (3)], we performed a least-squares fit of the Ar^{3+} cross section as a function of excess-energy range always starting at 0.0 eV and extending to an upper limit that increased in 0.25 eV steps. All three variables (σ_0, α, and C) were initially allowed to vary in the fit procedure.

By looking at how C varied as a function of excess-energy range, we determined a weighted average value for the background C. Once the background was determined, we performed a second fit to the Ar^{3+} cross section where C was fixed to the value determined in the previous fit.

In contrast to Ne (cf. Fig. 2), where σ_0 and α were free variables, the Ar fit of the same type did not reveal a clear picture of the energy dependence of the exponent α. The error bars were large for each value of the exponent and did not change appreciably from the initial value that we arbitrarily assigned to the exponent at the beginning of the fit, indicating that α and σ_0 were not sufficiently independent.

Therefore, we further confined the fit by allowing only the exponent α to vary. In order to do this, we had to determine the best average value for σ_0. We looked at the way σ_0 changed as a function of the upper limit of the fit range in the previously performed fit where only σ_0 and α were allowed to vary. We then took a weighted average of the values for σ_0 near threshold and used that value to constrain σ_0. We obtained $\sigma_0 = 67(5)$b for Ar, which is, unexpectedly, a factor of 10.5(1.3) larger than σ_0 for Ne. Taking into account the overall inaccuracy of the reported absolute cross sections for Ne and Ar, a systematic error of approximately 10% has to be added.

The modeling of α as a function of the upper limit of the fit range with σ_0 and C constrained is shown in Fig. 5. From this figure we conclude that the energy range of validity of the Wannier exponent for Ar is ~2.0 eV, which is markedly shorter than the ~5.0 eV range of validity for Ne. A fit of the Wannier exponent was performed from 0.0 to 2.0 eV (see Fig. 6), yielding the exponent $\alpha = 2.21(12)$, which again confirms the theoretical predicted value 2.162.

As in the case of Ne, another TPI threshold $[3p^3(^2D)]$ exists only 2.6 eV above the first threshold. While this energy appears to be close to the excess energy where the Wannier exponent is not valid anymore, the point for α at 2.6 eV in Fig. 5 clearly disagrees with the theoretical Wannier exponent, and the range of validity is indeed smaller than 2.6 eV. We believe that the approximate agreement of the second TPI threshold with the range of validity in Ne and Ar is merely fortuitous.

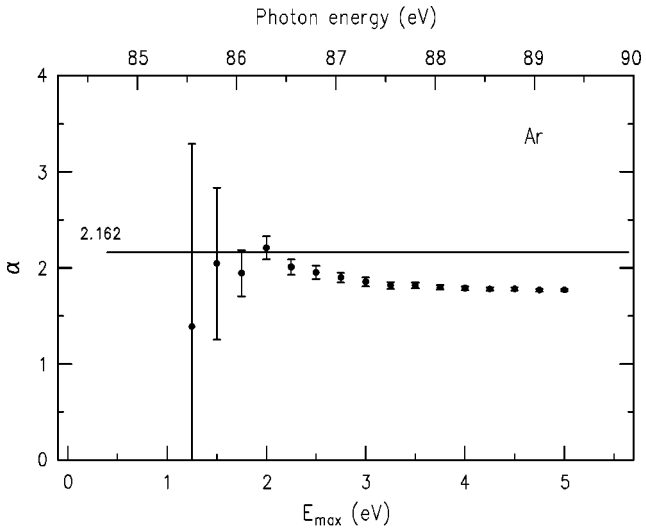

FIG. 5. The Wannier exponent as a function of the upper limit E_{max} of the energy range over which the fit was performed. The lower fit limit was fixed at 0 eV. The solid line indicates the theoretical value 2.162 of the Wannier exponent.

The reason why the Ar data needed to be further constrained than the Ne data is probably the difference in the energy range of validity of the Wannier exponent. Since the exponent decreases almost immediately above threshold in the Ar case, there are fewer data points in the power-law fit, which makes the problem of analyzing a system with multiple variables and relatively few data points near threshold statistically difficult.

VI. CONCLUSION

We have determined the triple-to-double and double-to-single photoionization ratios of Ne and Ar near the TPI

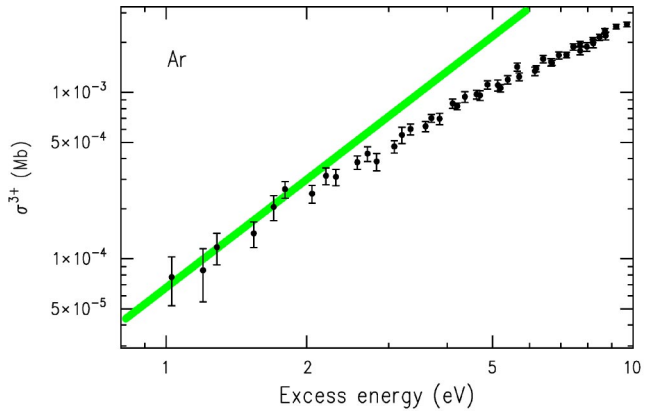

FIG. 6. Double-log plot of our Ar triple-photoionization cross section near threshold. The gray line corresponds to a power-law fit curve with an exponent of 2.21.

threshold. Using previous cross-section measurements [10], we derived the TPI cross section on an absolute scale.

In the case of Ne, we have confirmed the Wannier threshold law with an exponent of 2.20(5) for the first 5 eV above threshold in good agreement with previous measurements of Samson and Angel (2.17) [29] and confirm the theoretical predicted value of 2.162. We have also confirmed the exponent for the proposed second power law [29] when using the same energy range (5–9 eV) for the fit as in Ref. [29]. However, this value appears to be rather accidental since the exponent decreases gradually from 2.20 with increasing photon energy above 5 eV. From this we conclude that there is no physical significance to a second power law. Instead, the second exponent depends on the energy range over which the power law is applied. We have provided a dynamic way of looking at the exponent by making the upper energy limit of the fit a variable.

In addition, we have extended the near-threshold TPI investigations to Ar. From our Ar data we obtain an exponent of 2.21(12), which again confirms the theoretical Wannier exponent. However, we find a much shorter range of validity of the Wannier power law, namely, only 2 eV as compared to 5 eV in the case of Ne. The Wannier theory does not provide an energy range of validity, and the difference in the range of validity for various elements poses an interesting problem. Interestingly, we also found that the proportionality constant σ_0 is about a factor of 10 larger for Ar than for Ne. The TPI cross section near threshold is still unknown for many elements and further study of this process would give a better understanding of how the range of validity for the Wannier exponent changes.

ACKNOWLEDGMENTS

The authors wish to thank the SRC staff for excellent support. Financial support by the National Science Foundation (NSF) under Grant No. PHY-9987638 is gratefully acknowledged. One of us (D.L.) was partly supported by the Ministry of Science, Technology and Development of Serbia. The SRC is operated under NSF Grant No. DMR-0084402.

[1] T. N. Rescigno, M. Baertschy, W. A. Isaacs, and C. W. McCurdy, Science **286**, 2474 (1999).
[2] J. H. McGuire, N. Berrah, R. J. Bartlett, J. A. R. Samson, J. A. Tanis, C. L. Cocke, and A. S. Schlachter, J. Phys. B **28**, 913 (1995), and references therein.
[3] J. S. Briggs and V. Schmidt, J. Phys. B **33**, R1 (2000), and references therein.
[4] R. Wehlitz, M.-T. Huang, B. D. DePaola, J. C. Levin, I. A. Sellin, T. Nagata, J. W. Cooper, and Y. Azuma, Phys. Rev. Lett. **81**, 1813 (1998).
[5] R. Wehlitz, T. Pattard, M.-T. Huang, I. A. Sellin, J. Burgdörfer, and Y. Azuma, Phys. Rev. A **61**, 030704 (2000).
[6] R. B. Cairns, H. Harrison, and R. I. Schoen, Phys. Rev. **183**, 52 (1969).
[7] G. R. Wight and M. J. Van der Wiel, J. Phys. B **10**, 601 (1977).
[8] D. M. P. Holland, K. Codling, J. B. West, and G. V. Marr, J. Phys. B **12**, 2465 (1979).
[9] N. Saito and I. H. Suzuki, Int. J. Mass Spectrom. Ion Processes **115**, 157 (1992).
[10] I. H. Suzuki and N. Saito, Bull. Electrotech. Lab. (Tokyo, Japan, 1970-2001) **56**, 688 (1992).
[11] T. Matsuo, T. Hayaishi, Y. Itoh, T. Koizumi, T. Nagata, Y. Sato, E. Shigemasa, A. Yagishita, M. Yoshino, and Y. Itikawa, J. Phys. B **25**, 121 (1992).
[12] T. Nagata, Y. Itoh, T. Hayaishi, Y. Itikawa, T. Koizumi, T. Nagata, T. Matsuo, Y. Sato, E. Shigemasa, A. Yagishita, and M. Yoshino, J. Phys. B **22**, 3865 (1989).
[13] S. Baier, G. Gottschalk, T. Kerkau, T. Luhmann, M. Martins, M. Richter, G. Snell, and P. Zimmermann, Phys. Rev. Lett. **72**, 2847 (1994).
[14] T. Luhmann, Ch. Gerth, M. Martins, M. Richter, and P. Zimmermann, Phys. Rev. Lett. **76**, 4320 (1996).
[15] B. Kanngießer, W. Malzer, M. Müller, N. Schmidt, P. Zimmermann, A. G. Kochur, and V. L. Sukhorukov, Phys. Rev. A **68**, 022704 (2003).
[16] P. van Kampen, Ch. Gerth, M. Martins, P. K. Carroll, J. Hirsch, E. T. Kennedy, O. Meighan, J.-P. Mosnier, P. Zimmermann, and J. T. Costello, Phys. Rev. A **61**, 062706 (2000).
[17] G. H. Wannier, Phys. Rev. **90**, 817 (1953); **100**, 1180 (1954).
[18] G. H. Wannier, Phys. Rev. **100** 1180 (1955).
[19] H. Klar and W. Schlecht, J. Phys. B **9**, 1699 (1976).
[20] P. Grujić, J. Phys. B **16**, 2567 (1983).
[21] J. M. Feagin and R. D. Filipczyk, Phys. Rev. Lett. **64**, 384 (1990).
[22] K. A. Poelstra, J. M. Feagin, and H. Klar, J. Phys. B **27**, 781 (1994).
[23] M. Yu. Kuchiev and V. N. Ostrovsky, Phys. Rev. A **58**, 321 (1998).
[24] T. Pattard and J. M. Rost, Phys. Rev. Lett. **80**, 5081 (1998); **81**, 2618(E) (1998).
[25] V. N. Ostrovsky, Phys. Rev. A **64**, 022715 (2001).
[26] T. Pattard and J. M. Rost, Found. Phys. **31**, 535 (2001).
[27] A. Temkin and Y. Hahn, Phys. Rev. A **9**, 708 (1974).
[28] A. Temkin, Phys. Rev. Lett. **49**, 365 (1982); A. Temkin, in *Electronic and Atomic Collisions*, edited by J. Eichler, I. V. Hertel, and N. Stolterfoht (Elsevier, Amsterdam, 1984), pp. 755–765.
[29] J. A. R. Samson and G. C. Angel, Phys. Rev. Lett. **61**, 1584 (1988).
[30] H. Kossmann, V. Schmidt, and T. Andersen, Phys. Rev. Lett. **60**, 1266 (1988).
[31] R. Reininger, S. L. Crossley, M. A. Lagergren, M. C. Severson, and R. W. C. Hansen, Nucl. Instrum. Methods Phys. Res. A **347**, 304 (1994).
[32] R. K. Cole, F. K. Perkins, E. L. Brodsky, A. Filipponi, E. Korpella, D. C. Mancini, C. H. Pruett, D. J. Wallace, J. T. Welnak, and F. Zanini, Rev. Sci. Instrum. **60**, 2093 (1989).

[33] D. J. Wallace, G. C. Rogers, and S. L. Crossley, Nucl. Instrum. Methods Phys. Res. A **347**, 615 (1994).
[34] R. Wehlitz, D. Lukić, C. Koncz, and I. A. Sellin, Rev. Sci. Instrum. **73**, 1671 (2002).
[35] A. A. Radzig and B. M. Smirnov, *Reference Data on Atoms, Molecules, and Ions* (Springer Verlag, Berlin, Germany, 1985).
[36] G. C. King, M. Tronc, F. H. Read, and R. C. Bradford, J. Phys. B **10**, 2479 (1977).